Control and Cybernetics

vol. **32** (2003) No. 4

Modelling and identification of voids nucleation and growth effects in porous media plastic flow

by

Z. Nowak[1] **and A. Stachurski**[2]

[1] Institute of Fundamental Technological Research
Polish Academy of Sciences
Świętokrzyska 21, 00-049 Warsaw, Poland

[2] Institute of Control and Computation Engineering
Warsaw University of Technology
Nowowiejska 15/19, 00-665 Warsaw, Poland

Abstract: In the paper the effects of nucleation and growth of voids in the plastic porous media are investigated. Three different forms of the model are considered: the augmented Gurson model (total porosity model) with variable nucleation and growth material function, the same model with constant growth material function and the separated porosity model.

The identification of the material functions parameters is based on Fischer's experimental data set for axisymmetric tension of steel specimens and formulated as a typical nonlinear regression problem using the least squares approach. The resulting minimization problem is solved by means of our own implementation of the Boender at al. global minimization method.

Calculations and statistical analysis (Akaike, FPE and Vuong tests) have led to a conclusion that the growth material function in the uniaxial tension for steel may be assumed to be constant although not necessarily equal to one.

Keywords: plastic flow of voided media, material functions identification, global optimization, nonlinear regression, nonlinear programming, Akaike and FPE tests for nested models, Vuong test for nonnested models.

1. Introduction

In many mechanical problems of plastic flow and fracture of dissipative solids the intrinsic micro-damage effects are observed. Some researchers use a set of internal state variables to describe the intrinsic microdamage effects, while

others admit only one porosity parameter ξ and some material constants. We consider the latter way of description. In such constitutive models, in the form of the proposed evolution equation all parameters have to be determined. The evolution equation for the porosity parameter ξ has to describe the nucleation and growth mechanisms of microvoids.

The formation of microvoids in commercial grade materials is attributed to the presence of inhomogeneities which can be in the form of dispersed inclusions and/or second phases. The microvoids appear either as cracks in the particles or as failure of the particle-matrix interfacial bonding. The actual microvoid morphology depends upon the interrelation of various microstructural parameters as well as the local deformation state.

There have been many studies directed toward better understanding of void evolution and developing constitutive relations for inelastic porous solids. The model by Golganu et al. (1995), Søvik and Thaulow (1997), Pardoen and Delannay (1998), Pardoen, Doghri and Delannay (1998) and Pardoen and Hutchinson (2000), accounts for void shape effects and distribution of voids, respectively. In addition, some other effects, such as the strain mode effect in matrix (e.g. Koplik and Needleman, 1988; Tvergaard, 1990; Leblond et al., 1995; and Li et al., 2001) on the void growth, have been studied. All the analyses have shown clearly that besides the stress triaxiality and equivalent plastic strain, there are other effects influencing the growth of voids.

The volume fraction of microvoids ξ as a function of equivalent plastic strain $\bar{\epsilon}_p$ given by Fisher (1980) is plotted in Fig. 1. It should be stressed that Fisher's data are complete in that sense that they deliver not only the total porosity but also the nucleation part of porosity. In the first part of our calculations we have not exploited that information. Also the results presented in our earlier paper (Nowak and Stachurski, 2002) have used the total measure of porosity neglecting the rest of the experimental information. This is somehow justified because the majority of the experimental results available in the literature contains only measurements of the total porosity (see Needleman and Rice, 1978; Saje et al., 1982).

It is postulated that the evolution equation for porosity parameter has the form (see Needleman and Rice, 1978; Perzyna, 1984; or Perzyna and Nowak, 1987)

$$\begin{aligned} (\dot{\xi}) &= (\dot{\xi})_{\text{nucleation}} + (\dot{\xi})_{\text{growth}} = \\ &= \tilde{h}(\bar{\epsilon}_p, \xi)\boldsymbol{\sigma} : \boldsymbol{D}^p + \tilde{g}(\bar{\epsilon}_p, \xi)\boldsymbol{D}^p : \boldsymbol{I} \end{aligned} \tag{1}$$

where $\tilde{h}$, $\tilde{g}$ are the material functions, $\boldsymbol{I}$ denotes the unit tensor, $\bar{\epsilon}_p$ is the equivalent plastic strain, $\boldsymbol{\sigma}$ is the Cauchy stress tensor, $\boldsymbol{D}^p$ denotes the plastic rate of the deformation tensor and the operator: means the trace of second order tensors.

It is assumed that the nucleation mechanism occurs mainly at second-phase

particles, by decohesion of the particle-matrix interface and by the particle cracking. The growth process is postulated to be controlled only by the plastic flow phenomenon. Both assumptions are justified by the experimental observation results for metals (see a review paper by Needleman and Rice, 1978).

The first term in the evolution equation (1) for the porosity parameter ξ describes debonding of second-phase particles from the matrix as the plastic work progressively increases. The nucleation material function $\tilde{h}$ depends on the equivalent plastic deformation $\bar{\epsilon}_p$ and the porosity ξ. The second term in Eq. (1) is related to the growth mechanism. It is assumed that the growth material function $\tilde{g}$ also depends on the equivalent plastic deformation $\bar{\epsilon}_p$ and the porosity ξ.

In this paper we focus on the identification of material functions with the Fisher's (1980) experimental data. Some parts of our work parallel and extend what has been carried out by Perzyna and Nowak (1987) and by Nowak and Stachurski (2001, 2002). All of them focus on the total porosity model. In paper one only theoretical total porosity model has been proposed. Two last papers document its numerical verification with various variants of material functions. In the current paper we propose another model with separated nucleation and growth effects, carry out numerical identification of both models and compare the results.

We consider the separate evolution equations for the voids growth and the voids nucleation, i.e. we used the model in the form of two differential evolution equations with two state variables (growth of volume of fraction of voids and nucleation fraction of voids). We have assumed the additivity of the two kinds of porosity components. Therefore in the right hand sides of the two differential equations appear sum of the porosity components (see equation 12). The model and the appropriate mean square functional for that case are presented in Section 4.

The Gurson's voided media plastic flow model itself is a set of differential equations (equilibrium, constitutive, plastic flow and porosity evolution equations). The involvement of the Bridgman's equilibrated solution for the stress state reduces this set to one differential equation. To obtain the calculated porosity parameter, ξ, in the first case, we had to solve poorly conditioned differential evolution equation (1). The second case involves a set of two ordinary differential equations.

The material function formulae used in the first case are described and the corresponding resulting least squares problem is introduced in Section 5. Data used for parameter estimation are presented in Section 6. The computational results are shown and discussed in Section 7. Some conclusions and observations are also stated. In Tables 1a, 2a, 3a the "best" minima found for each interval are collected. The presentation of the whole set of local minima is restricted to three sectors due to the lack of space (see Tables 1a, 2a and 3a). Section 8 is devoted to the analysis of the identification results. Finally, Section 9 contains some concluding remarks.

In this paper we focus on the traditional least squares formulation (see for example Levenberg, 1944; Marquardt, 1963) of the identification problem, where the sum of the second powers of deviations of the calculated and measured values is minimized. We have expected existence of many local minima in our problem. Therefore we have used our own implementation of the global minimization procedure of Boender at al.in the form presented in Törn and Žilinskas (1989) in standard ANSI C language. It combines the clusterization approach with local minimization. Locally, we have used the BFGS quasi-Newton method with the numerical gradient estimation (see for instance Bazaraa et al., 1993; Bertsekas, 1997; Fletcher, 1987; Stachurski and Wierzbicki, 2001). The BFGS method is an unconstrained optimization method; however, in our implementation we have introduced box constraints on the parameters. Differential equations have been solved by means of the Rosenbrock method for stiff differential equations (see Press et al., 1993). Details of the implementation can be found in Nowak and Stachurski (2001).

2. Porosity model in the case of total porosity

2.1. Porosity evolution at the neck

In the following considerations the uniaxial test is carried out in the room temperature. At the neck there exists a complex state of stress and maximum deformations. A material point is identified by the Cartesian convected coordinates x^i $(i = 1, 2, 3)$ in the reference state. In the current deformed state the coordinates of the material point, relative to the Cartesian frame, are denoted by $\bar{x}^i$. We assume, following Chakrabarty (2000), that after a neck has been formed in a cylindrical tensile specimen, the distribution of the stress across a transverse section is not uniform. We have assumed an augmented version of the Gurson's (1977) porous material model with the following porosity evolution

$$\dot{\xi} = h(\bar{\epsilon}_p)\frac{1}{1-\xi}tr(\boldsymbol{\sigma}\boldsymbol{D}^p) + g(\bar{\epsilon}_p)(1-\xi)tr(\boldsymbol{D}^p). \tag{2}$$

It is the Gurson's form of the equation of porosity evolution with varying $g(\bar{\epsilon}_p)$ as proposed by Perzyna (1984). Non constant $g(\bar{\epsilon}_p)$ reflects the influence of voids from the neighbourhood on the growth of a particular void. In equation (2) the plastic strain controlled nucleation criterion suggested by Gurson's (1977) analysis of experimental data obtained by Gurland (1972) is assumed. The nucleation of microvoids is not dependent on the hydrostatic stress. We assume that $h(\bar{\epsilon}_p)$ and $g(\bar{\epsilon}_p)$ are functions depending on plastic strain and unknown parameters.

Our purpose is to determine the material functions $h(\bar{\epsilon}_p)$ and $g(\bar{\epsilon}_p)$ on the basis of the total porosity experimental data set. We have tested many formulae for $h(\bar{\epsilon}_p)$ and $g(\bar{\epsilon}_p)$, described in Section 5.

We have assumed the following form of the evolution equation (2) for a porous plastic solid

$$\frac{\dot{\xi}}{\dot{\bar{\epsilon}}_p} = \left[h \frac{1}{1-\xi} \left(\lambda_1 \frac{\sigma_{xx}}{\sigma_{zz}} + \lambda_2 \frac{\sigma_{yy}}{\sigma_{zz}} + 1 \right) + g(1-\xi)(\lambda_1 + \lambda_2 + 1) \right] \frac{1}{\sqrt{\lambda^*}} \quad (3)$$

where $\lambda_1 = \dfrac{\dot{E}^p_{xx}}{\dot{E}^p_{zz}}$, $\lambda_2 = \dfrac{\dot{E}^p_{yy}}{\dot{E}^p_{zz}}$ and $\lambda^* = \frac{2}{3}[(\lambda_1)^2 + (\lambda_2)^2 + 1]$, $\dot{x}i$ is the derivative of the porosity, $\dot{\bar{\epsilon}}_p$ is the derivative of the equivalent plastic strain. $\dot{E}^p_{xx}$, $\dot{E}^p_{yy}$ and $\dot{E}^p_{zz}$ are the plastic rates of the deformation tensor components in the Cartesian x, y and z coordinates.

2.2. Stress state at the neck

We employ Bridgman's (1952) solution for the stress state at the center of the minimum section of the tensile cylindrical sample. It has been obtained due to the assumption of the uniform deformation of the elements in the minimum section implying that the circumferential strain rate $\dot{E}_{yy}$ is equal to radial strain rate $\dot{E}_{xx}$ in the minimum section (see Chakrabarty, 2000, p.161). Inserting this equality in the equilibrium equations and combining with the yield condition yields

$$\begin{aligned} \sigma_{xx} &= \sigma_{yy} = \bar{\sigma} \ln \left(\frac{1}{2} \frac{R}{\rho_R} + 1 \right) \\ \sigma_{zz} &= \bar{\sigma} \left(1 + \ln \left(\frac{1}{2} \frac{R}{\rho_R} + 1 \right) \right) \end{aligned} \qquad \text{for } \; x,\; y,\; z = 0. \quad (4)$$

The analytical expression for the stress depends on the matrix flow stress, $\bar{\sigma}$ and the geometry of the neck, i.e. on the ratio $\frac{R}{\rho_R}$, where R is the radius of the minimum section and ρ_R is the neck contour radius. The behaviour of the matrix material is represented by a piecewise power law of the form $\bar{\sigma} = \sigma_y \cdot (\bar{\epsilon}_p/\epsilon_y)^N$, σ_y is the yield stress in uniaxial tension, ϵ_y is the yield strain of the matrix material and N is the matrix strain hardening exponent, e.g. for carbon steel σ_y=175.0 MPa, ϵ_y= 0.001 and N= 0.18. Similarly as in Saje, Pan and Needleman (1982) it is assumed that

$$\begin{aligned} \frac{R}{\rho_R} &= 0.833(\bar{\epsilon}_p - 0.18), \qquad && \text{for} \quad \bar{\epsilon}_p \geq 0.18 \\ \frac{R}{\rho_R} &= 0.0, && \text{for} \quad \bar{\epsilon}_p < 0.18\,. \end{aligned} \quad (5)$$

Taking equation (5) into account in the Bridgman's solution we obtain for axisymmetric tension

$$\frac{\sigma_{xx}}{\sigma_{zz}} = \frac{\sigma_{yy}}{\sigma_{zz}} = \lambda \tag{6}$$

where

$$\lambda = \ln\left(\frac{1}{2}\frac{R}{\rho_R} + 1\right) / \left(1 + \ln\left(\frac{1}{2}\frac{R}{\rho_R} + 1\right)\right). \tag{7}$$

Furthermore, we have assumed the constitutive relation for the porous plastic solids introduced by Gurson (1977). This constitutive relation can be put into the form introduced by Rudnicki and Rice (1975), $\dot{E}_{ij} = \frac{1}{H} P_{ij} Q_{kl} \overset{\triangledown}{\sigma}{}^{kl}$, where $\overset{\triangledown}{\boldsymbol{\sigma}}$ is the Jaumann rate-of-change of Cauchy stress tensor. Using this relation we can determine λ_1 and λ_2

$$\lambda_1 = \lambda_2 = (3S_{xx} + \bar{\sigma}\alpha)/(3S_{zz} + \bar{\sigma}\alpha) \tag{8}$$

where $S_{ij} = \sigma_{ij} - \frac{1}{3}\sigma_{kk}\delta_{ij}$ and

$$\alpha = \xi \sinh(\frac{\sigma_{kk}}{2\bar{\sigma}}). \tag{9}$$

3. Formulation of the identification problem in the case of total porosity

The problem considered in the current section has been reformulated. Our task is to find the optimal estimates of the unknown parameters in the material functions $h(\bar{\epsilon}_p)$ and $g(\bar{\epsilon}_p)$ which appear in equation (1). It is assumed that the nucleation mechanism in (1)is controlled by the plastic strain only. The identification problem is stated as the problem of finding values of the material function parameters ensuring minimal value of the mean square functional calculated as the sum of the second powers of differences between the observed output values Y_i and corresponding calculated output values $\tilde{Y}_i$ ($\tilde{Y}_i = F(\bar{\epsilon}_{pi}, x)$). Here F represents the assumed model. It connects the input independent variable values, $\bar{\epsilon}_{pi}$, with the output values, ξ, and accordingly x denotes the unknown parameters. Thus, our problem is

$$\min_{x \in V} \|\boldsymbol{Y} - \tilde{\boldsymbol{Y}}\|^2 \tag{10}$$

where $V \subset R^n$ denotes the set of admissible parameters values (n is the number of the unknown parameters to be identified). Substitution of the formula $\tilde{Y}_i = F(\bar{\epsilon}_{pi}, x)$ into (10) yields

$$\min_{x \in V} \sum_{i=1}^{M} \left\{Y_i - F(\bar{\epsilon}_{pi}, x)\right\}^2 . \tag{11}$$

The second term in formula (11) represents the calculated output values $\tilde{Y}_i$, and M is the number of observations (measured input and corresponding output values). In (11), the second power of the euclidean distance is used. If $V = R^n$ (the unconstrained case), the minimization of the distance is equivalent to the minimization of its second power. Therefore, in the least squares method usually the second power of the distance in the observations space is minimized.

In our primal problem the calculated output is obtained as a result of the integration of an ordinary differential equation, where on the left-hand side its derivative with respect to the input $\bar{\epsilon}_p$ appears. The right-hand side of the differential equation depends on the input and output variables and on unknown parameters. The unknown parameters appear exclusively in the so-called material functions being a part of the right-hand side of the differential equation. See for details Sections 2 and 5.

The parameters should belong to the set V of feasible values of parameters, defined in Section 5. In this part we have not made any use of the data on the growth or nucleation volume fractions although they are available in the Fisher's data set.

4. Formulation of the identification problem in the case of separated nucleation and growth porosity

Identification of parameters in the formulation stated in Section 3 suggested that there exists an intrinsic non-uniqueness in the parameter determination. It has led to the observation that material functions h and g in some sense mutually compensate their impact on the identified model.

Our first trial to eliminate that phenomenon was use of $g \equiv 1$. We have carried out several identification runs with $g = 1$ and various variants of h.

The second trial tested by us was the explicit use of the full Fisher's data set taking into account not only the values of the total porosity but also the corresponding separated nucleation and the growth porosity. We have changed accordingly the identified model to the form of two separate evolution equations – the first one describing the nucleation of new voids and the second one describing growth of the already existing voids. Those differential evolution equations are mutually connected by introduction of the total porosity into their right-hand sides as follows

$$\begin{aligned} \dot{\xi}^n &= h(\bar{\epsilon}_p)\tfrac{1}{1-\xi^n-\xi^g} tr(\boldsymbol{\sigma}\boldsymbol{D}^p) \\ \dot{\xi}^g &= g(\bar{\epsilon}_p)(1-\xi^n-\xi^g) tr(\boldsymbol{D}^p) \quad . \end{aligned} \tag{12}$$

This means that we keep the additivity assumption saying that total porosity ξ is the sum of the nucleation and growth effects, i.e. $\xi = \xi^n + \xi^g$. The model represented by equations (12) is not mathematically equivalent to the model (2). Anyhow, we believe that it is justified on the basis of the existing models describing separately the phenomena of nucleation of new voids and growth of

existing voids. The only difference is the replacement of the partial ξ on the right-hand sides by the total porosity.

The above presented change in the model formulation is reflected in the mean square function (11) where instead of the sums of squares of deviations of the measured and calculated total porosity we sum up the squares of deviations of the measured and calculated nucleation part of porosity ξ^n and the squares of deviations of the measured and calculated growth porosity ξ^g, respectively

$$\min_{x\in V}\left[\sum_{i=1}^{M}\left\{\bar{\xi}_i^n-\xi^n(\bar{\epsilon}_{pi},x)\right\}^2+\sum_{i=1}^{M}\left\{\bar{\xi}_i^g-\xi^g(\bar{\epsilon}_{pi},x)\right\}^2\right]. \tag{13}$$

Here, $\bar{\xi}^n$ and $\xi^n(\bar{\epsilon}_{pi},x)$ denote the experimental and calculated (for given parameters x) values of the nucleation of new voids, and $\bar{\xi}^g$ and $\xi^g(\bar{\epsilon}_{pi},x)$ denote the experimental and calculated values of the growth of existing voids, respectively. The calculated values $\xi^n(\bar{\epsilon}_{pi},x)$ and $\xi^g(\bar{\epsilon}_{pi},x)$ are obtained by the numerical integration of the differential evolution equations (12).

We have used the same sets of material functions as in the previous two parts of our identification calculations.

5. Material functions

This section contains formulae of the material functions which we have used for identification. There exist certain requirements that the shape of the material function h has to satisfy. We started trying to follow the ideas of Chu and Needleman (1980). So, as the first type of the function, the Gauss normal distribution function for function h was applied

$$h_1(\bar{\epsilon}_p,a_1,b_1,c_1)=\frac{a_1}{b_1\sqrt{2\pi}}\exp\left(-\frac{1}{2}\left[\frac{\bar{\epsilon}_p-c_1}{b_1}\right]^2\right). \tag{14}$$

where a_1,b_1,c_1 are the unknown parameters. All of these parameters have their mechanical meaning. Namely, a_1 denotes the maximum value of the porosity parameter, b_1 is the width of the voids distribution region and c_1 represents the value of the equivalent plastic strain $\bar{\epsilon}_p$ at the moment when the porosity parameter reaches its maximal value.

We have also used two other forms of the material functions h

$$h_2 = a_1(\bar{\epsilon}_p)^{b_1}\exp(c_1\bar{\epsilon}_p) \tag{15}$$

$$h_3 = a_1[1+\tanh(b_1\bar{\epsilon}_p+c_1)]. \tag{16}$$

The second material function g describing the growth of microvoids must be uniformly equal to 1 when the initial void or voids are isolated in an unbounded matrix. It means that voids do not interact, no nucleation of new voids and no coalescence of voids in the growth process are considered. These three phenomena are closely interrelated and can occur simultaneously. In our analysis

this function g is not necessarily constant. As a first form of the g function the following formula (as in Perzyna and Nowak, 1987) was used

$$g_1(\bar{\epsilon}_p, a_2, b_2, c_2) = a_2 \exp\left[b_2 \left(\bar{\epsilon}_p\right)^{c_2}\right] . \tag{17}$$

Unfortunately, in this case, the mechanical interpretation of the unknown parameters a_2, b_2 and c_2 is not so clear.

The identification was also carried out with five other different forms of the material function g, namely

$$g_2 = a_2\sqrt{(\bar{\epsilon}_p)^2 + b_2(\bar{\epsilon}_p) + c_2} \tag{18}$$

$$g_3 = \frac{a_2}{b_2 - \bar{\epsilon}_p} \tag{19}$$

$$g_4 = 1 \tag{20}$$

$$g_5 = a_2 \tag{21}$$

$$g_6 = a_2 + b_2 \cdot \bar{\epsilon}_p . \tag{22}$$

Tables 1a summarizes case notation for the total porosity model and Table 1b for the separated porosity model. For instance Case A1 denotes selection of h_1 and g_1. This means that we apply the Gauss normal distribution function as the nucleation material function h and exponential function as the growth material function g. Case B1 corresponds to h_2 and g_1, and so on.

Table 1a. Summary of notations for the total porosity model

	g-function					
	g_1	g_2	g_3	g_4	g_5	g_6
h_1	A1	A2	A3	A4	A5	A6
h_2	B1	B2	B3	B4	B5	B6
h_3	C1	C2	C3	C4	C5	C6

The corresponding cases for the separated porosity model are denoted similarly. The only difference is the addition of capital D in front of the case symbol. Hence, for example DA1 means the use of functions h_1 and g_1.

Table 1b. Summary of notations for the separated porosity model

	g-function					
	g_1	g_2	g_3	g_4	g_5	g_6
h_1	DA1	DA2	DA3	DA4	DA5	DA6
h_2	DB1	DB2	DB3	DB4	DB5	DB6
h_3	DC1	DC2	DC3	DC4	DC5	DC6

We have maintained the same order of notations in the separated and total porosity models to simplify the comparison of identification results in both cases. The tables of results for the total porosity model are presented in the Appendix subsection A1 and for the separated porosity model in subsection A2.

6. Brief description of Fisher's data used for estimation

In J.R. Fisher's experimental investigation two carbon steels with 0.17 (type B) and 0.44 (type W) weight percent carbon, respectively, were used for the quantitative studies of microvoid nucleation and growth. All testing was done at the room temperature. Metallographic observations were made on both undeformed and deformed specimens using both optical and electron microscopy. For each specimen, a series of transverse sections was prepared corresponding to successively smaller axial distances from the minimum cross section. Each new section was obtained by grinding to the next premarked position and thus the previous sections were destroyed. Therefore, all data required from a given section had to be obtained before preparation of the succeeding one. Each section was carefully polished and etched after preliminary use of various grades of abrasive papers. The microstructural parameters were determined in both deformed and undeformed specimens. For the deformed specimens the areal density of voids, η_A, and the volume fraction of voids, ξ, were obtained from transverse sections by standard metallographic techniques performed on scanning electron micrographs taken at a magnification of 2000 times. It is observed in Fisher's experiment that the voids tended to have elliptical cross sections similar to those of the particles, as might be expected since the particles were nucleation sites for these voids.

The total volume fraction of voids, ξ, and the nucleation part of volume fraction of voids, ξ^n, obtained by Fisher (1980) are plotted as the function of equivalent plastic strain $\bar{\epsilon}_p$ in Fig. 1. This measure of voids is used in our analysis in Section 4, with separation of the nucleation part from the full measure of ξ. As in Perzyna and Nowak (1987) the resulting diagrams of the nucleation part of ξ^n and the growth part of ξ^g versus $\bar{\epsilon}_p$ are shown also in Fig. 1.

In this work, the thorough analysis of the data set was omitted since we decided to concentrate on the computational aspects of the problem of parameter estimation. We were interested in the question of whether it is in fact the global optimization problem. Furthermore, we wanted to obtain the decisive answer to the question of whether the assumed model does fit at all the given data set.

7. Numerical results

In this section the results of parameter estimation are presented. It is impossible to present all aspects of the calculations in a short paper. Therefore we restrict the presentation of the minima found to just the three with the smallest mean square function values.

Our aim in considering various forms of material functions was to obtain the "best" fitting of the model to the data in the sense of finding the parameters ensuring the smallest value of the mean square functional (11) or (13), respectively. Furthermore, in all cases it is necessary to impose some bounds on the parameters to assure their appropriate mechanical interpretation and to avoid

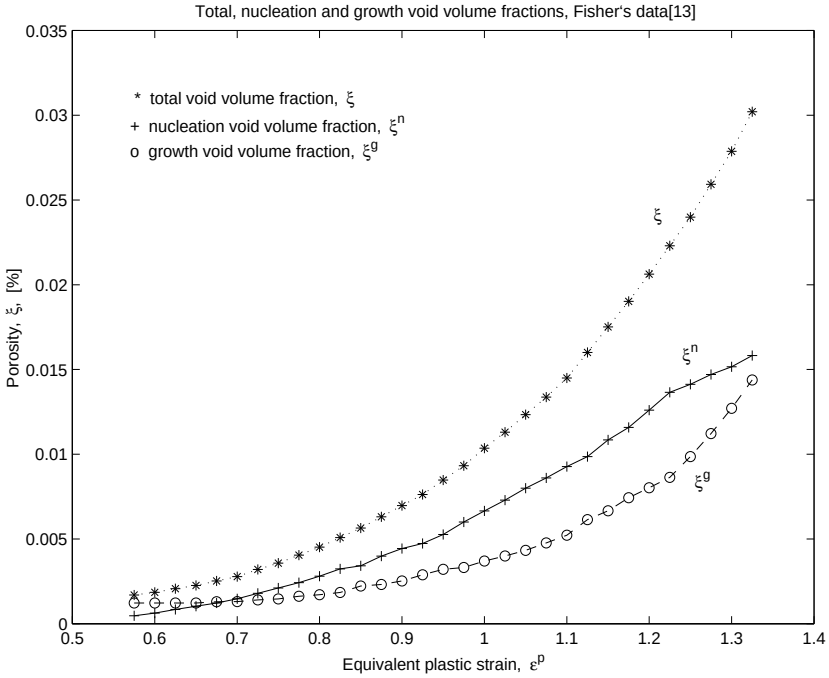

Figure 1. Total void volume fraction, ξ, the nucleation volume void fraction, ξ^n (data from Fisher, 1980, for the B1 type steel) and the calculated growth volume void fraction, ξ^g, as a function of equivalent plastic strain, $\bar{\epsilon}_p$.

overflows in calculations (specially for the g function). In our computations we have used the following strategy – at the beginning a broad range of the feasible parameters were assumed. Next, we have continued our calculations taking at the subsequent steps small intervals containing the previously found optimal values of parameters as their new feasible ranges. At each such main step we have found several local optima. For many of them the underlying variables were located at the range bounds. Because of that we have adopted special strategy consisting in subsequent minimizations with restricted range of parameters. It gave us an opportunity to better explore the whole range of parameters we were interested in. The second and very important reason for such strategy was the large computational effort and memory requirements for storing many local minima and points leading towards them if we decided to run the program assuming excessively broad range of parameters. The third and not less important reason were numerical difficulties encountered in the integration of the differential equation. Its right-hand side contains a singularity and is very sensitive even with respect to relatively small changes in some parameters. It was sometimes impossible to satisfy the accuracy requirements in the double

precision arithmetic of the workstation.

In each case we have started our computations assuming at the beginning a broad range of feasible parameters. For instance in Cases A1, A2 and A3 we have taken

A1:	0.01	$\le a_1 \le$	0.05,	0.1	$\le b_1 \le$	0.6,	0.9	$\le c_1 \le$	1.3
	1.0	$\le a_2 \le$	1.5,	0.01	$\le b_2 \le$	0.3,	0.01	$\le c_2 \le$	0.6
A2:	0.01	$\le a_1 \le$	0.1,	0.1	$\le b_1 \le$	0.5,	1.0	$\le c_1 \le$	1.3
	0.1	$\le a_2 \le$	0.6,	0.5	$\le b_2 \le$	1.2,	0.8	$\le c_2 \le$	1.8
A3:	0.01	$\le a_1 \le$	0.1,	0.1	$\le b_1 \le$	1.0,	1.0	$\le c_1 \le$	1.3
	1.5	$\le a_2 \le$	3.0,	2.5	$\le b_2 \le$	5.0			

The results are presented in Appendix in subsections A1 and A2, in Tables 2a, 2b–5a, 5b. Tables with suffix "a" contain the following information about a minimum:

- the corresponding values of parameters
- the functional values f.

Tables with suffix "b" contain frequently used statistical information:

- residual standard deviation $\boldsymbol{s_e}$, where

$$\boldsymbol{s_e}^2 = \frac{\left[\sum_{i=1}^{M}(Y_i - \tilde{Y}_i)^2\right]}{M} \tag{23}$$

where: M is the number of observations, Y_i are the observed values of the output, $\tilde{Y}_i$ are the calculated values of the output

$$\tilde{Y}_i = F(\bar{\epsilon}_{p^i}, x) \text{ for } i = 1, \ldots, M \tag{24}$$

- relative standard error s_{ew}

$$s_{ew} = \frac{s_e}{\bar{Y}} \tag{25}$$

where $\bar{Y}$ is the mean value of the observed output

$$\bar{Y} = \frac{\left[\sum_{i=1}^{M} Y_i\right]}{M} \tag{26}$$

- correlation coefficient $r_{Y\tilde{Y}}$ between the observed and calculated output:

$$r_{Y\tilde{Y}} = \frac{\sum_{i=1}^{M}\left(Y_i - \bar{Y}_i\right)\left(\tilde{Y}_i - \bar{\tilde{Y}}\right)}{\left[\sum_{i=1}^{M}\left(Y_i - \bar{Y}\right)^2\right]^{\frac{1}{2}}\left[\sum_{i=1}^{M}\left(\tilde{Y}_i - \bar{\tilde{Y}}\right)^2\right]^{\frac{1}{2}}} \tag{27}$$

where $\bar{\tilde{Y}}$ is the mean value of the calculated output

$$\bar{\tilde{Y}} = \frac{\left[\sum_{i=1}^{M} \tilde{Y}_i\right]}{M} \tag{28}$$

- Akaike's information criterion AIC (Söderström and Stoica, 1989, p. 442, eq. 11.48; Holnicki et al., 2000, pp. 187-189)

$$\boldsymbol{AIC} = M * \ln V_M(\hat{x}) + 2 * n \tag{29}$$

where n denotes the number of the model parameters and $V_M(\hat{x})$ is the loss function

- final prediction error criterion (FPE) (Söderström and Stoica, 1989, p. 444, eq. 11.54; Holnicki at al., 2000, pp. 187-189)

$$\boldsymbol{FPE} = V_M(\hat{x}) * \frac{1 + n/M}{1 - n/M}. \tag{30}$$

In the cases with the prefix "D" corresponding to the model with the separated nucleation and growth porosity all statistical quantities except for the Akaike's and FPE information criteria are duplicated, i.e. they are given separately for the nucleation and growth values. Akaike and FPE information criteria are calculated for the separated cases treated as total (i. e. after summing up the outputs) to make them comparable with the total cases. Those criteria are used for discriminating between the rival nested models. Further, we use only part of them in the analysis because only few of our models form groups of nested models.

Tables are organized as follows. Subsection A1 contain the results for the total porosity model – in Tables 2 with variable growth material function, in Tables 3 with constant growth material function. Similarly, in subsection A2 we present the results for the separate porosity model, again presented in two groups – in Tables 4 with variable growth material function and in Tables 5 with constant growth material function.

7.1. Vuong test for discriminating between the rival nonnested models

There exist several tests for discriminating between the nonnested models (for instance: Cox test, Vuong test, Bayes factors, F test, J test, JA test) (see Clarke, 2000; McAleer, 1995; Vuong, 1989). We have considered the use of the Cox and Vuong Tests. The Cox test is harder to perform than the Vuong test. It requires many extra simulations to calculate its value. Furthermore, it may reject both of the two compared models without any decision. The Vuong test is the easiest to perform; it is only necessary to calculate the difference in the average log-likelihoods and calculation of the normalization. It requires neither

simulation nor any prior information. Vuong test nether leaves us without any answer. It allows to select the best model even from a set of bad nonnested models.

The null hypothesis in the Vuong test is that compared models $\mathcal{M}_1$ and $\mathcal{M}_2$ are equivalent. The H_1 hypothesis states that model $\mathcal{M}_1$ is better than $\mathcal{M}_2$, while H_2 hypothesis is that model $\mathcal{M}_1$ is worse than $\mathcal{M}_2$. The actual (approximate) test is:

$$\text{under } H_0 : \frac{LR_M(\hat{\theta}^1_M, \hat{\theta}^2_M)}{(\sqrt{M}) \cdot \hat{\omega}_M} \longrightarrow N(0,1) \tag{31}$$

$$\text{under } H_1 : \frac{LR_M(\hat{\theta}^1_M, \hat{\theta}^2_M)}{(\sqrt{M}) \cdot \hat{\omega}_M} \longrightarrow +\infty \tag{32}$$

$$\text{under } H_2 : \frac{LR_M(\hat{\theta}^1_M, \hat{\theta}^2_M)}{(\sqrt{M}) \cdot \hat{\omega}_M} \longrightarrow -\infty \tag{33}$$

where

$$LR_M(\hat{\theta}_1, \hat{\theta}^2_M) \equiv L^1_M(\hat{\theta}^1_M) - L^2_M(\hat{\theta}^2_M) \tag{34}$$

$$\hat{\omega}^2_M \equiv \frac{1}{M} \sum_{i=1}^{M} \left[\ln \frac{f_1(Y_i|X_i; \hat{\theta}^1_M)}{f_2(Y_i|Z_i; \hat{\theta}^2_M)} \right]^2 - \left[\frac{1}{M} \sum_{i=1}^{M} \ln \frac{f_1(Y_i|X_i; \hat{\theta}^1_M)}{f_2(Y_i|Z_i; \hat{\theta}^2_M)} \right]^2 . \tag{35}$$

Here $L^1_M(\hat{\theta}^1_M)$ is the logarithm of the likelihood function for model $\mathcal{M}_1$ with the parameters $\hat{\theta}^1_M$ and $L^2_M(\hat{\theta}^2_M)$ is the logarithm of the likelihood for model $\mathcal{M}_2$ with the parameters $\hat{\theta}^2_M$, respectively (for the definition of likelihood function see e.g. Söderström and Stoica, 1989).

The symbol $f_1(Y_t|X_t; \hat{\theta}^1_M)$ ($f_2(Y_t|X_t; \hat{\theta}^2_M)$) denotes the likelihood function for the model $\mathcal{M}_1$ ($\mathcal{M}_2$) with parameters equal to $\hat{\theta}^1_M$ ($\hat{\theta}^2_M$) – the estimated values of the unknown parameters θ.

In simple terms, if the null hypothesis is true, the average value of the log-likelihood ratio should be zero. If the H_1 hypothesis is true, the average value of the log-likelihood ratio should be significantly greater than zero. If the reverse is true, the average value of the log-likelihood ratio should be significantly smaller than zero. This means that the Vuong test statistic is simply the average log-likelihood ratio suitably normalized.

Our models have different number of parameters. Therefore, following Clarke (2001) we have adjusted the log likelihood ratio statistic

$$\widehat{\mathrm{LR}}_M(\hat{\theta}^1_M, \hat{\theta}^2_M) = \mathrm{LR}_M(\hat{\theta}^1_M, \hat{\theta}^2_M) - \left[\left(\frac{n1}{2} \right) \ln(n1) - \left(\frac{n2}{2} \right) \ln(n2) \right] \tag{36}$$

where $n1$ and $n2$ are the numbers of parameters in models 1 and 2, respectively.

This adjusted value has been used to calculate Vuong test results collected in Tables 6, 7 and 8. Table 6 contains the results of the mutual comparison of models A1, A2, A3, A6, B1, B2, B3, B6, C1, C2, C3, C6 and Table 7 – of models DA1, DA2, DA3, DA6, DB1, DB2, DB3, DB6, DC1, DC2, DC3, DC6. Models represented in Table 8 were selected according to the following rules:

- select on the basis of the Akaike or FPE information criteria (Tables 2b, 3b, 4b and 5b) the best model from any group with $g \equiv 1$, g being the estimated constant and g linear and one particular form of the h function, for instance A4, A5 and A6
- select using the Vuong criterion (Tables 6 and 7) the best representative of any group with one h formula and all other forms of g including linear g (for instance, the first group consists of A1, A2, A3 and A6)
- Models selected in two previous steps are compared via the Vuong test (the results of the pairwise comparison are collected in Table 8).

8. Analysis of the identification results

We have carried out four separate variants of numerical experiment. The first one concerned the case of the total porosity model and variable shape of both material functions. The results are collected in Tables 2a and 2b. In the second case we have assumed constant growth material function g (we have tested two variants – the first one with $g = 1$ and the second one with an estimated value of that constant). Those results may be found in Tables 3a and 3b, respectively. Similar two cases have been used for the model with separate porosity. The results for varying shape of g are presented in Tables 4a and 4b and the corresponding results for constant g in Tables 5a and 5b. We have used various forms of material functions. Therefore the above mentioned cases contain many subcases. We have found many local minima in all subcases. Their presentation in Tables 2a–5a is restricted to the best three of them, ordered with respect to the fitting error values in the increasing order. Tables 2b–5b contain the corresponding statistical indicators. The results presented in tables show the variety of possible solutions to the minimization of the mean squares function if the parameters appear in the model nonlinearly. It seems that the presented numerical results justify the hypothesis that many local minima exist in the considered problem. Many of the local minima found are acceptable also from the statistical point of view.

The values of $r_{Y\bar{Y}}$ close to 1 show a good correlation between the calculated and measured output.

Tables 2a and 2b contain the computational and statistical results for the estimation with the varying growth function g. Fig. 2 presents the corresponding dependence of the total porosity differences (observed minus calculated values) on the equivalent plastic strain. The analysis of Tables 2a and 2b shows that for the varying growth material function g the worst choice of the nucleation material function h is the powered exponent function (15). Two other nucleation

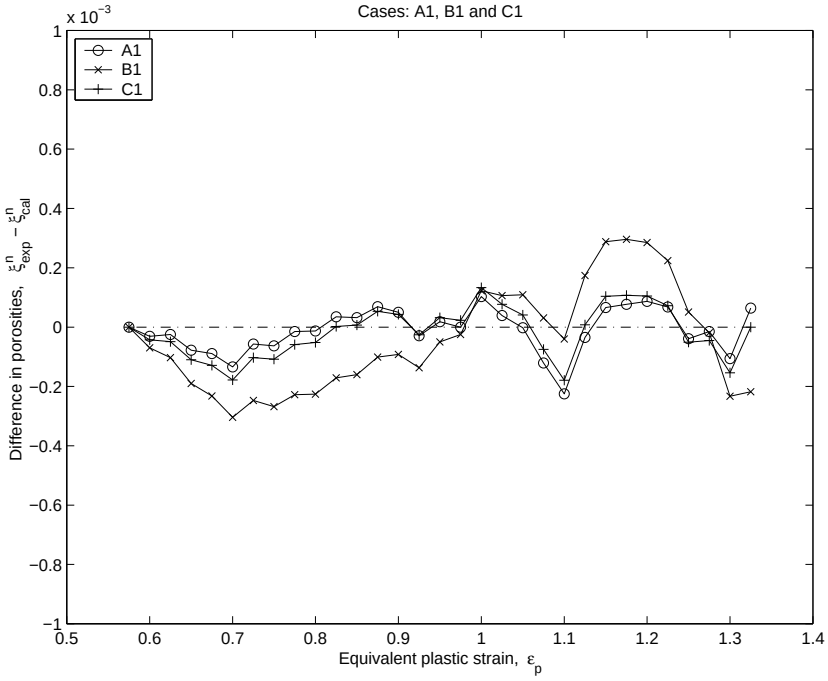

Figure 2. Differences between the experimental and calculated total porosity for cases A1, B1, C1, A2, B2 and C2 versus equivalent plastic strain with varying g.

material functions – normal distribution function (14) and shifted hyperbolic tangent function (16) are equally good. The mechanical interpretation of the normal distribution function parameters is easier. It was frequently used in the previous studies published in the literature. Therefore in our opinion the normal distribution nucleation material function is a reasonable choice.

The large number of local minima found in all cases from that group led us to the conclusion that there exists a kind of internal nonuniqueness in the total porosity model. Due to that observation we have decided to study the total porosity model with the constant g material function (with $g \equiv 1$), i.e. the form of the porosity model proposed by Gurson (1977).

The results accumulated in Tables 3a and 3b show that fitting error is of the same magnitude as in the corresponding cases with varying g function. Statistical indicators are not worse than in cases with varying growth function g. Fig. 3 presents the resulting dependence of the total porosity differences (observed minus calculated values) on the equivalent plastic strain in the case of constant g.

The results collected in Tables 3a and 3b for the constant growth function g suggest that the estimated constant value of g is preferred as compared to the

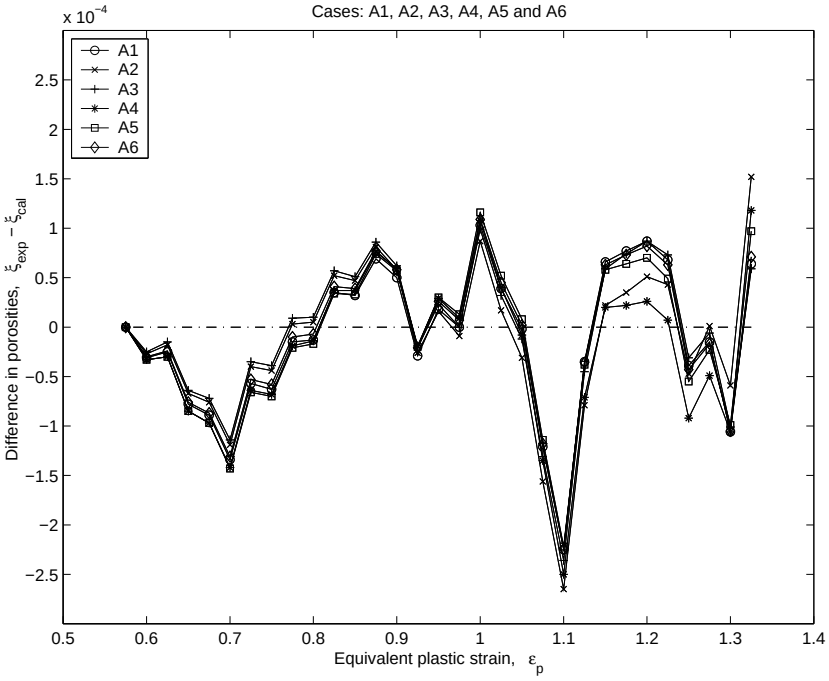

Figure 3. Differences between the experimental and calculated total porosity for cases A4, B4, C4, A5, B5 and C5 versus equivalent plastic strain for constant g.

constant $g \equiv 1$. We can derive also the same conclusion as for the varying growth function g – namely that the powered exponent nucleation function h is the worst choice. The conclusions drawn on the basis of the fitting error agree with those deduced from the Akaike and FPE test values. In group A (with h being the Gauss function) the best one among A4, A5 and A6 is A5, in group B – B5 and in group C – C4. For the separated case Akaike and FPE point out that linear g (i.e. DA6, DB6 and DC6) are the best ones in all three groups.

Vuong test (Tables 6 and 7) selects A3 (from A1-A3 and A6), B3 (from B1-B3 and B6) and C6 (from C1-C3 and C6). The best models selected by means of the Akaike and FPE tests for each group and those selected by means of the Vuong test were further compared using again the Vuong test (see Table 8). The analysis of Table 8 shows that the best choice is the shifted hyperbolic tangent as the h function and $g \equiv 1$ (model C4). Similarly good results are obtained with the Gauss normal distribution as the h function and g – an estimated constant. The fitting error is better for model A5.

To conclude the presentation of the results for the total porosity model we have included Figs. 4 (a - b) containing graphs of material functions h (for the models C4 and A5) showing the dependence of their values on the equivalent

plastic strain. Second possibility of overcoming the nonuniqueness studied by us

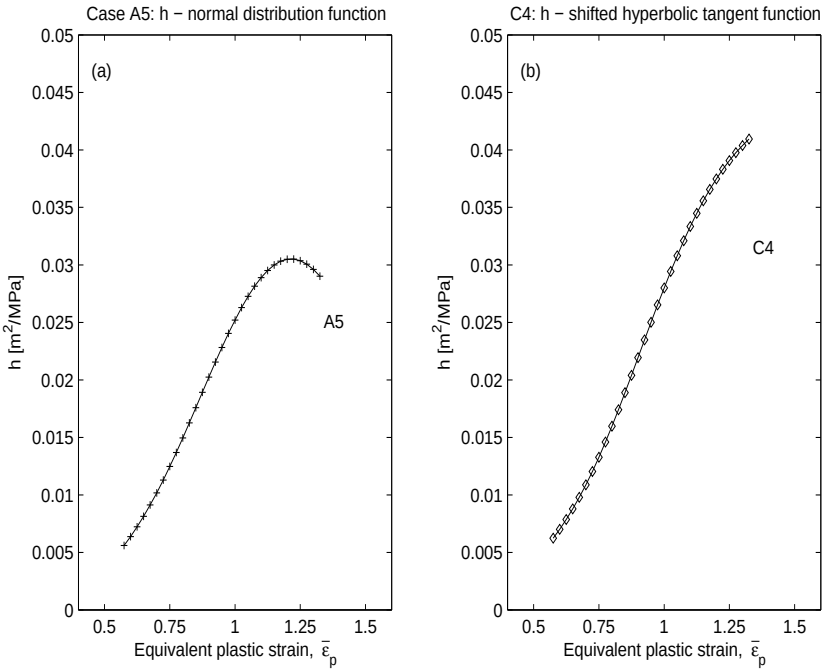

Figure 4. Graphs of the material functions values for the total porosity model, *a*) model A5 and *b*) model C4, versus the equivalent plastic strain.

was the investigation of the separated model. It was possible to pose the problem in that way because Fisher's data contain the total and nucleation parts of porosity separately. The total porosity models considered by us assume the additivity of these two phenomena – growth and nucleation of voids. However, when separate data are available, it seems to be natural to exploit them separately in the model and in the corresponding identification problem. This is exactly what we have done in cases DA, DB and DC. We have formulated the separate porosity model and identified its parameters. The results are collected in Tables 4a–5b. The fitting error is in that case of magnitude 10^{-6} and the statistical indicators are also relatively good. It should be stressed, however, that the fitting error in that case is the sum of deviations of two outputs – nucleation and porosity growth.

The computations have been carried out in the similar manner as in the total porosity model. We have started with the varying growth function g and afterwards continued with the constant growth material function g.

The estimated results for the varying growth function are collected in Table 4a and the corresponding statistical indicators in Table 4b. Fig. 5 presents

the resulting dependence of the total porosity differences (observed minus calculated values) with respect to the equivalent plastic strain. General conclusion

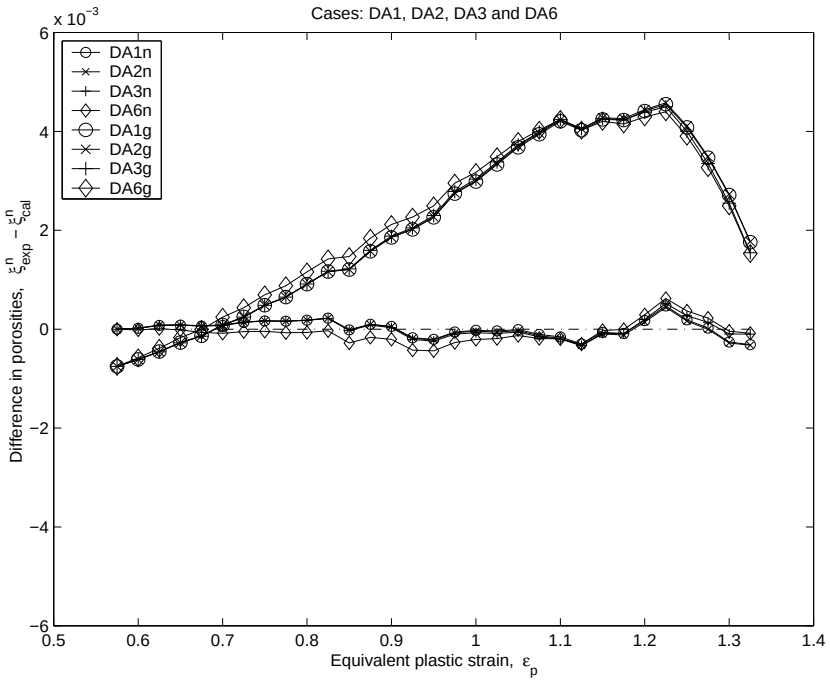

Figure 5. Differences between the experimental and calculated separated porosity for cases DA1, DA2, DB1, DB2, DC1 and DC2 versus equivalent plastic strain with varying g.

is the same as for the total porosity model. The powered exponential function h is the worst choice. The normal distribution and the shifted hyperbolic tangent functions are almost equally good. Therefore we recommend the use of the normal distribution functions since it is easier to interpret its parameters and it is more frequently used. Furthermore, the graph of the growth function g is approximately linear (see Figure 7). Therefore we have tried also the linear form of g, obtaining only slightly larger fitting error.

We have tried also to use the constant growth material function g. The results are collected in Tables 5a and 5b. Fig. 6 presents the resulting dependence of the total porosity differences (observed minus calculated values) with respect to the equivalent plastic strain. The fitting errors are quite small in that case. Also correlations between the calculated and observed porosity are acceptable. It is interesting in that case that the Vuong test prefers model DC6 (g is linear), but the material function g is almost constant, although not equal to 1. Its value is approximately equal to 0.86. We have observed a strong tendency

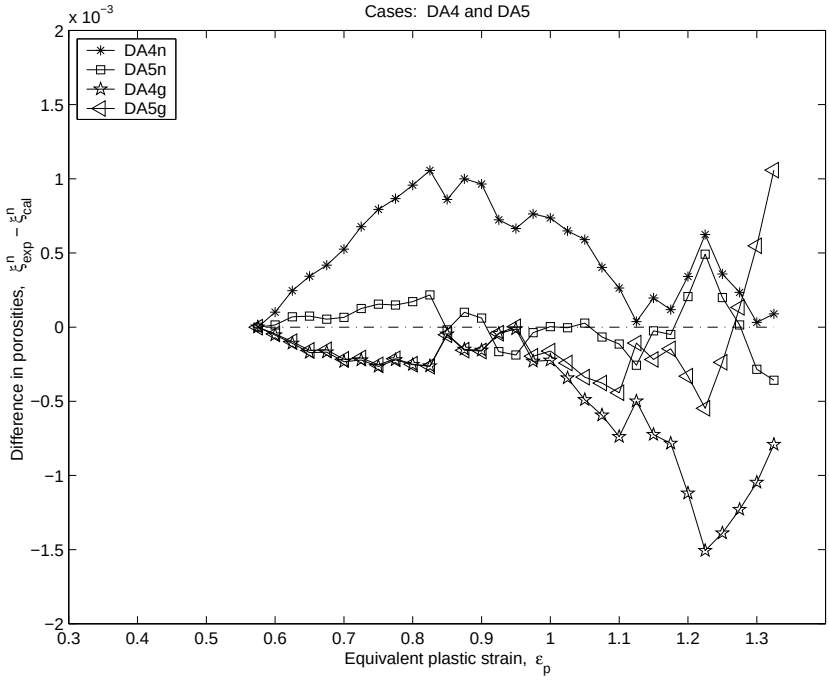

Figure 6. Differences between the experimental and calculated separated porosity for cases DA4, DA5, DB4, DB5, DC4 and DC5 versus equivalent plastic strain with constant g.

towards that constant value. Even in other local minima found, the estimated constant value of g is almost equal to 0.86. Such phenomenon was not so clearly observed in the total porosity model although the Vuong test value shows that the model C4 is the best one and the model A5 (with h – the Gauss normal distribution function and g – an estimated constant) is only a bit worse. The value of the Vuong test of order 10^{-3} permits even to claim that C4 and A5 are equivalent.

Figs. 7 a,b contain graphs of the material functions $DA5$ and $DC6$ showing the dependence of their values with respect to the equivalent plastic strain.

9. Conclusions and comments

The main novelty of the paper lies in the introduction of the model with separated nucleation and growth of voids. This differentiates substantially the current paper from its two predecessors (Nowak and Stachurski, 2001, 2002), where we have considered exclusively the model with total porosity. In the current investigation we have identified the material functions parameters for

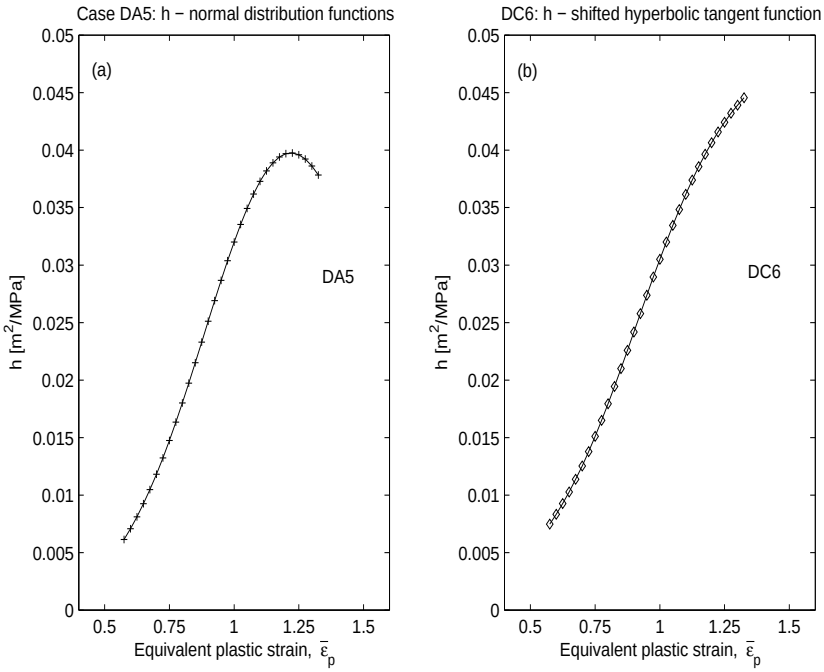

Figure 7. Graphs of the material functions values for the separated porosity model, *a*) model DA5 and *b*) model DC6, versus the equivalent plastic strain.

both variants of the model with various forms of the material functions. Special attention has been paid to the case with constant function g (with an estimated constant value and its case with $g = 1$). The identification results were analysed and compared. We have included also statistical tests for discrimination of the nested models (Akaike and FPE information criteria) and the Vuong test for nonnested models selection.

It should be stressed that in the identification process of the model with separated porosity the minimized mean squares function (11) consists of two summarized terms. In the first one we sum up the squares of deviations of the measured and calculated nucleation part of porosity ξ^n and in the second term the squares of deviations of the measured and calculated growth porosity ξ^g, respectively.

The estimated material functions h (for the best models) are plotted in Fig. 4 for the total porosity model and in Fig. 7 for the separate porosity model. We would like to stress that our material function was determined with following important assumptions. The matrix material is plastically incompressible ($\dot{\rho}_m = 0$ where ρ_m is matrix density) and the elastic part of a strain rate tensor is neglected, $D_{ij} = D^p_{ij}$. All our conclusions concern exclusively the ductile steel

material, although qualitative conclusions may be valid also for other types of materials.

We have found several local minima in all cases. The best fitting error for the total porosity model is of order 10^{-7}. However, fitting error in other cases is only slightly larger. Of course, the corresponding material function parameters have different values.

In all tested forms of the separated models we have also found several sets of parameters (local minima of the mean square function) with the fitting errors close to the best one (within the range from 10^{-6} to 10^{-5}). The parameters are reasonable from the mechanical point of view. An interesting and open question is which local minimum found should be selected. It seems that in the total porosity model (when the voids nucleation and growth phenomena are simultaneously present), the constant material function $g \equiv 1$ as used by many researchers is a reasonable choice. However, we should stress that the identification procedure with $g = a_2$, where parameter a_2 was identified, has led to a bit different value of that constant – in the total porosity model approximately equal to 0.9 and in the separate porosity model approximately equal to 0.86. In our opinion the value 0.86 obtained for the separate porosity model is probably closer to the real value since in this model we have exploited the available experimental data more thoroughly.

In the separate porosity model the fitting error is of the order of 10^{-6}. However, in this case the mean squares function has a double number of the summed components (60 versus 30 in the total porosity cases). In fact, we sum up the fitting errors for the nucleation and growth porosity parts. Having that in mind, we may claim that the separate porosity model is at least as good as the best total porosity model. In our opinion it is even better to apply the separate porosity model for voids nucleation and growth processes in the elastic–plastic material subject to a unidirectional elongation.

Our numerical experiments suggest that the nucleation of new voids can be modelled using the normal distribution material function. This choice was among the best in all tested cases. We have observed equally good results for the shifted hyperbolic tangent function. We recommend the use of the normal distribution function because it is easier to interpret its parameters in mechanical terms. In view of our results it is reasonable to use the porosity model with a constant value of the growth material function g, though with the constant not equal to 1. For the ductile steel this constant is probably near 0.86.

In our opinion the results obtained are very interesting. They indicate that while modelling jointly the nucleation and growth of voids it is reasonable to use the total porosity model with constant material function g. However, contrary to the common practice it seems that the constant should be different from the usually applied value 1. We suggest its identification for each particular material.

The formulation of the minimized function is an open question. It is not clear

whether the euclidean distance in the space of observations is the best measure. One can use in the formula (10) the l_1–norm or l_∞–norm or any other suitable norm. Then the problem will be nondifferentiable and will have completely different features but it can also be handled by our computational program after a replacement of the local gradient minimizer by a suitable nondifferentiable optimization method. It is the next possibility we intend to study in the future – the use of other measures of deviations of the calculated output from the measured one. Existence of many local minima is also expected in that case.

The work of Z. Nowak has been prepared in part within the framework of the research project KBN 8T07A 05221.

The work of A. Stachurski has been sponsored by the Faculty of Electronics and Information Technology, Warsaw University of Technology, under the Dean's Grant No. 50960013003.

References

Bazaraa, M.S., Sherali, J. and Shetty, C.M. (1993) *Nonlinear Programming. Theory and Algorithms.* John Wiley and Sons, New York, Chichester, Brisbane, Toronto.

Bertsekas D.P. (1997) *Nonlinear Programming.* Athena Scientific, Massachussets.

Boender, C.G., Rinnooy Kan, A.H.G., Strougie, L. and Timmer, G.T. (1982) A Stochastic Method for Global Optimization. *Mathematical Programming* **22**, 125-140.

Bridgman, P.W. (1952) *Studies in Large Plastic Flow and Fracture.* McGraw-Hill.

Chakrabarty, J. (2000) *Applied Plasticity.* Springer-Verlag, New York.

Clarke, K.A. (2001) Testing nonnested models of international relations: reevaluating realism. *American Journal of Political Science* **45** (3), http://citeseer.nj.nec.com/445599.html.

Fisher, J.R. (1980) *Void nucleation in spheroidized steels during tensile deformation.* Ph.D. Thesis, Brown University.

Fletcher, R. (1987) *Practical Methods of Optimization* (second edition). John Wiley & Sons, Chichester.

Gologanu, M., Leblond, J.-B., Perrin, G. and Devaux, J. (1995) Recent extensions of Gurson's model for porous ductile metals. In: P. Suquet, ed., *Continuum Micromechanics.* Springer, Berlin, 61–130,

Gurson, A.L. (1977) Continuum theory of ductile rupture by void nucleation and growth. Part 1. Yield criteria and flow rules for porous ductile media. *J. Engng. Materials and Technology, Trans. of the ASME* **99**, 2–15.

GURLAND, J. (1972) Observations on the fracture of cementite particles in spheroidized 1.05%C steel deformed at room temperature. *Acta Metall.* **20**, 735–741.

HOLNICKI, P., NAHORSKI, Z., and ŻOCHOWSKI, A. (2000) *Modelling Natural Environment Processes.* (Modelowanie Procesów Środowiska Naturalnego, in Polish). Wyższa Szkoła Informatyki Stosowanej i Zarządzania, Warsaw.

KOPLIK, J. and NEEDLEMAN, A. (1988) Void growth and coalescence in porous plastic solids. *Int. J. Solids Structure* **24**, 835–853.

LEBLOND, J.-B., PERRIN, G. and DEVAUX, J. (1995) An improved Gurson-type model for hardenable ductile metals. *European Journal of Mechanics & Solids* **14**, 499–527.

LEVENBERG, K. (1944) A Method for the Solution of Certain Nonlinear Problems in Least Squares. *Quart. Appl. Math.* **2**, 164–168.

LI, G.C., LING, X.W. and SHEN, H. (2001) On the mechanism of void growth and the effect of straining mode in ductile materials. *Int. J. Plasticity* **16**, 39–58.

MARQUARDT, D.W. (1963) An Algorithm for Least Squares Estimation of Nonlinear Parameters. *SIAM Journal on Applied Mathematics* **11**, 431–441.

MCALEER, M. (1995) The significance of testing empirical non-nested models. *Journal of Econometrics* **67**, 149–171.

NEEDLEMAN, A., RICE, J.R. (1978) Limits to ductility set by plastic flow localization. In: N.-M. Wang, ed., *Mechanics of Sheet Metal Forming.* Plenum, New York, 237–267.

NOWAK, Z. and STACHURSKI, A. (2001) Nonlinear regression problem of material functions identification for porous media plastic flow. *Engineering Transactions* **49**, 637–661.

NOWAK, Z., STACHURSKI, A. (2002) Global optimization in material functions identification for voided plastic flow. *Computer Assisted Mech. Engng Sciences* **9**, 205–221.

PARDOEN, T. and DELANNAY, F. (1998) Assessment of void growth models from porosity measurements in cold-drawn copper bars. *Metallurgical and Materials Transactions* **29A**, 1895–1909.

PARDOEN, T., DOGHRI, I. and DELANNAY, F. (1998) Experimental and numerical comparison of void growth models and void coalescence criteria for the prediction of ductile fracture in copper bars. *Acta Materialia* **46**, 541–552.

PARDOEN, T. and HUTCHINSON, J.W. (2000) An extended model for void growth and coalescence. *Journal Mech. Phys. Solids* **48**, 2467–2512.

PERZYNA, P. (1984) Constitutive modelling of dissipative solids for postcritical behaviour and fracture. *ASME J. Engng. Mater. Technol.* **106**, 410–419.

Perzyna, P. and Nowak, Z. (1987) Evolution equation for the void fraction parameter in necking region. *Arch. Mech.* **39** (1–2), 73–84.

Press, W.H., Teukolsky, S.A., Vetterling, W.T. and Flannery, B.P. (1993) *Numerical Recipes in C: The Art of Scientific Computing*. Cambridge University Press, Cambridge.

Rudnicki, J.W. and Rice, J.R. (1975) Conditions for the localization of deformation in pressure-sensitive delatant materials. *Journal Mech. Phys. Solids* **23**, 371–394.

Saje, M., Pan, J. and Needleman, A. (1982) Void nucleation effects on shear localization in porous plastic solids. *Int. J. Fracture* **19**, 163.

Søvik, O.P. and Thaulow, C. (1997) Growth of spherical void in elastic-plastic solids. *Fatigue Fract. Engng Mater. Struct.* **20** (12), 1731–1744.

Söderström, T. and Stoica, P. (1989) *System Identification*. Prentice Hall, International University Press, Cambridge.

Stachurski, A. and Wierzbicki, A.P. (2001) *Introduction to Optimization*, (Podstawy Optymalizacji, in Polish), second edition. Oficyna Wydawnicza Politechniki Warszawskiej, Warsaw.

Törn, A. and Žilinskas, A. (1989) *Global Optimization*. Springer Verlag, Berlin, Heidelberg.

Tvergaard, V. (1990) Material failure by void growth to coalescence. *Adv. Appl. Mech.* **27**, 83–151.

Vuong, Q. (1989) Likelihood ratio tests for model selection and nonnested hypothesis. *Econometrica* **57**, 307–333.

APPENDIX

A1. Results for total porosity model

A.1.1 Results for total porosity model with variable growth material function

Table 2a. Identified parameters and fitting errors for the cases A1–A3, A6, B1–B3, B6, C1–C3, C6

h - nucleation functions with a_1, b_1 and c_1;
g - growth functions with a_2, b_2 and c_2

	Case	a_1	b_1	c_1	a_2	b_2	c_2	f
1		2.081212e-2	3.203613e-1	1.142677	1.048110	1.540339e-1	5.887020e-1	1.700284e-7
2	A1	2.459752e-2	3.417624e-1	1.193470	1.100321	6.501482e-2	1.941033e-1	1.870735e-7
3		2.073352e-2	3.246460e-1	1.146024	1.052570	1.627909e-1	1.541159e-1	2.013667e-7
4		2.819688e-2	3.290185e-1	1.187475	5.039920e-1	1.021578	1.688143	1.893821e-7
5	A2	2.794326e-2	3.427333e-1	1.193001	5.362410e-1	1.092745	1.430616	1.984865e-7
6		3.177080e-2	3.360531e-1	1.216207	4.689406e-1	1.144043	1.563800	2.007179e-7
7		2.412438e-2	3.145564e-1	1.148306	2.461575	3.356563		1.662608e-7
8	A3	2.687249e-2	3.690178e-1	1.200510	2.393928	3.208201		4.727793e-7
9		3.609856e-2	3.933141e-1	1.275095	2.547901	3.755815		1.028279e-6
10		2.563980e-2	3.317624e-1	1.178424	7.627987e-1	3.095568e-1		1.695705e-7
11	A6	1.862920e-2	2.969529e-1	1.091176	7.654488e-1	4.380955e-1		2.032952e-7
12		1.286682e-2	2.446338e-1	1.003067	8.499793e-1	4.991069e-1		2.139974e-7
13		1.548730e-2	1.829196	5.966584e-1	8.291838e-1	7.157868e-2	2.912159e-1	1.007905e-6
14	B1	1.642854e-2	1.897919	6.861903e-1	6.229555e-1	1.044736e-1	3.917156e-1	1.164333e-6
15		1.294056e-2	1.607321	6.287958e-1	9.292985e-1	1.462683e-1	2.302958e-1	1.471906e-6
16		1.634198e-2	1.747208	6.708150e-1	3.888362e-1	8.832497e-1	1.310916	1.390740e-6
17	B2	1.698248e-2	1.715469	6.782495e-1	3.606531e-1	7.974402e-1	1.143107	2.038704e-6
18		1.431830e-2	1.570579	7.059013e-1	4.823660e-1	7.234962e-1	1.288154	2.177861e-6
19		1.584352e-2	1.903237	8.008182e-1	2.024103	4.653833		9.331585e-7
20	B3	1.381212e-2	1.690606	8.287273e-1	2.167394	4.049697		1.225122e-6
21		1.425329e-2	1.933893	8.256529e-1	2.266634	4.265744		2.052942e-6
22		1.479078e-2	1.666422	7.552346e-1	5.761520e-1	1.418413e-1		1.535279e-6
23	B6	1.505820e-2	1.575890	6.345494e-1	4.726391e-1	3.762108e-1		1.588777e-6
24		1.300701e-2	1.504593	7.394732e-1	4.973083e-1	4.156869e-1		1.954040e-6
25		2.455850e-2	2.586369	-2.422738	8.068700e-1	1.790121e-1	2.790432e-1	2.300857e-7
26	C1	2.682353e-2	2.564554	-2.452859	7.687302e-1	1.746709e-1	1.753534e-1	2.645276e-7
27		2.934788e-2	2.423116	-2.400235	7.755841e-1	1.312077e-1	2.187021e-1	2.910709e-7
28		2.858736e-2	2.722919	-2.550194	4.112641e-1	8.034553e-1	1.506650	1.887593e-7
29	C2	2.461063e-2	2.757709	-2.492385	4.711461e-1	6.901616e-1	1.561727	2.070639e-7
30		2.621142e-2	2.710815	-2.496059	4.430647e-1	8.500000e-1	1.574596	2.211636e-7
31		3.995557e-2	2.536548	-2.595604	1.795428	4.213291		2.207438e-7
32	C3	3.997300e-2	2.646143	-2.670479	1.517623	3.966418		2.565705e-7
33		3.724288e-2	2.823082	-2.764387	1.419700	3.752633		3.545108e-7
34		2.980778e-2	2.684975	-2.562633	5.488091e-1	2.078393e-1		1.977660e-7
35	C6	2.846895e-2	2.812794	-2.622759	4.963934e-1	2.529827e-1		1.984614e-7
36		2.912654e-2	2.806816	-2.626160	4.518431e-1	2.739501e-1		2.009751e-7

Table 2b. Statistical results for the cases A1–A3, A6, B1–B3, B6, C1–C3, C6

s_e – standard deviation, s_{ew} – relative standard error, $r_{Y\tilde{Y}}$ – correlation coefficient, *Akaike* – AIC information-criterion, FPE – Final Prediction Error information criterion

	Case	s_e	s_{ew}	$r_{Y\tilde{Y}}$	Akaike	FPE
1		5.667615e-9	6.572061e-3	9.999637e-1	-5.776599e+2	8.117485e-9
2	A1	6.235784e-9	6.884115e-3	9.999638e-1	-5.746983e+2	8.931251e-9
3		6.712223e-9	7.138756e-3	9.999649e-1	-5.724159e+2	9.613636e-9
4		6.312736e-9	6.935533e-3	9.999592e-1	-5.743181e+2	9.041468e-9
5	A2	6.616216e-9	7.087291e-3	9.999649e-1	-5.728625e+2	9.476130e-9
6		6.690596e-9	7.147402e-3	9.999548e-1	-5.725159e+2	9.582661e-9
7		5.542027e-9	6.502675e-3	9.999630e-1	-5.803546e+2	7.426041e-9
8	A3	1.575931e-8	1.092479e-2	9.999182e-1	-5.479574e+2	2.111669e-8
9		3.427596e-8	1.597171e-2	9.999392e-1	-5.238699e+2	4.592809e-8
10		5.652350e-9	6.564784e-3	9.999631e-1	-5.797435e+2	7.573868e-9
11	A6	6.776505e-9	7.175781e-3	9.999612e-1	-5.741204e+2	9.080183e-9
12		7.133247e-9	7.384449e-3	9.999521e-1	-5.725300e+2	9.558197e-9
13		3.359683e-8	1.595189e-2	9.998283e-1	-5.224903e+2	4.811934e-8
14	B1	3.881109e-8	1.699830e-2	9.998880e-1	-5.180178e+2	5.558751e-8
15		4.906353e-8	1.923160e-2	9.997048e-1	-5.107511e+2	7.027164e-8
16		4.635799e-8	1.860863e-2	9.998255e-1	-5.125095e+2	6.639662e-8
17	B2	6.795680e-8	2.240796e-2	9.998653e-1	-5.006527e+2	9.733167e-8
18		7.259538e-8	2.318532e-2	9.997187e-1	-4.986058e+2	1.039753e-7
19		3.110528e-8	1.532762e-2	9.998493e-1	-5.268790e+2	4.167954e-8
20	B3	4.083740e-8	1.757314e-2	9.997854e-1	-5.184402e+2	5.472009e-8
21		6.843140e-8	2.293090e-2	9.995485e-1	-5.024369e+2	9.169468e-8
22		5.117596e-8	1.951984e-2	9.998754e-1	-5.114444e+2	6.857326e-8
23	B6	5.295923e-8	1.991955e-2	9.997619e-1	-5.103825e+2	7.096274e-8
24		6.513467e-8	2.216006e-2	9.995955e-1	-5.039676e+2	8.727722e-8
25		7.669524e-9	7.641082e-3	9.999525e-1	-5.682828e+2	1.098474e-8
26	C1	8.817585e-9	8.173929e-3	9.999543e-1	-5.639585e+2	1.262906e-8
27		9.702364e-9	8.609684e-3	9.999510e-1	-5.609943e+2	1.389629e-8
28		6.291975e-9	6.924098e-3	9.999600e-1	-5.744202e+2	9.011734e-9
29	C2	6.902130e-9	7.247827e-3	9.999590e-1	-5.715510e+2	9.885631e-9
30		7.372120e-9	7.483696e-3	9.999561e-1	-5.695089e+2	1.055878e-8
31		7.358126e-9	7.489766e-3	9.999517e-1	-5.715678e+2	9.859525e-9
32	C3	8.552350e-9	8.079605e-3	9.999423e-1	-5.669053e+2	1.145972e-8
33		1.181703e-8	9.511706e-3	9.999218e-1	-5.568819e+2	1.583423e-8
34		6.592200e-9	7.091104e-3	9.999561e-1	-5.749752e+2	8.833221e-9
35	C6	6.615379e-9	7.105462e-3	9.999555e-1	-5.748664e+2	8.864281e-9
36		6.699170e-9	7.149989e-3	9.999549e-1	-5.744762e+2	8.976555e-9

A.1.2 Results for total porosity model with constant growth material function

Table 3a. Identified parameters and fitting errors for the cases A4, A5, B4, B5, C4, C5

h - nucleation functions with a_1, b_1 and c_1;

g - constant growth function with $a_2 = 1$ and a_2 estimated

	Case	a_1	b_1	c_1	a_2	f
1		3.505692e-2	3.666815e-1	1.282348	1.0	1.983268e-7
2	A4	3.065935e-2	3.348365e-1	1.227703	1.0	2.887013e-7
3		3.100329e-2	3.470957e-1	1.232653	1.0	4.546674e-7
4		2.657334e-2	3.473849e-1	1.214838	1.142003	1.788396e-7
5	A5	2.447573e-2	3.233043e-1	1.178914	1.134999	2.451784e-7
6		3.740360e-2	3.533577e-1	1.278640	9.023870e-1	2.818601e-7
7		1.226463e-2	1.502548	7.367378e-1	1.0	1.360788e-6
8	B4	1.248952e-2	1.485976	7.146476e-1	1.0	1.442864e-6
9		1.277779e-2	1.465261	6.870349e-1	1.0	1.612120e-6
10		1.329750e-2	1.628454	7.325886e-1	9.028104e-1	1.162902e-6
11	B5	1.358028e-2	1.577733	6.369864e-1	9.849008e-1	1.364839e-6
12		1.327030e-2	1.430378	6.405346e-1	1.002564	2.077057e-6
13		2.261183e-2	2.727299	-2.484556	1.0	1.974333e-7
14	C4	2.296294e-2	2.671381	-2.452580	1.0	2.105957e-7
15		2.265837e-2	2.685177	-2.450903	1.0	2.123488e-7
16		2.424185e-2	2.816120	-2.586525	9.380108e-1	1.913195e-7
17	C5	2.255315e-2	2.781891	-2.528091	9.999952e-1	1.975519e-7
18		2.868764e-2	2.618190	-2.527397	8.544051e-1	2.025599e-7

Table 3b. Statistical results for the cases A4, A5, B4, B5, C4, C5

s_{ew} – standard deviation, s_{ew} – relative standard error, $r_{Y\tilde{Y}}$ – correlation coefficient, *Akaike* – AIC information-criterion, FPE – Final Prediction Error information criterion

	Case	s_{e}	s_{ew}	$r_{Y\tilde{Y}}$	Akaike	FPE
1		6.610892e-9	7.091231e-3	9.999589e-1	-5.788874e+2	7.768561e-9
2	A4	9.623375e-9	8.571815e-3	9.999349e-1	-5.672477e+2	1.130858e-8
3		1.515558e-8	1.071005e-2	9.999251e-1	-5.531683e+2	1.780955e-8
4		5.961321e-9	6.740050e-3	9.999619e-1	-5.800937e+2	7.478358e-9
5	A5	8.172614e-9	7.880864e-3	9.999507e-1	-5.703133e+2	1.025238e-8
6		9.395336e-9	8.464723e-3	9.999369e-1	-5.659911e+2	1.178626e-8
7		4.535961e-8	1.840385e-2	9.998250e-1	-5.191844e+2	5.330276e-8
8	B4	4.809546e-8	1.893327e-2	9.998404e-1	-5.173689e+2	5.651771e-8
9		5.373734e-8	1.998720e-2	9.998534e-1	-5.139304e+2	6.314756e-8
10		3.876339e-8	1.707357e-2	9.998541e-1	-5.220560e+2	4.862792e-8
11	B5	4.549464e-8	1.852984e-2	9.998501e-1	-5.170923e+2	5.707212e-8
12		6.923523e-8	2.261579e-2	9.998598e-1	-5.040749e+2	8.685424e-8
13		6.581110e-9	7.078005e-3	9.999598e-1	-5.790274e+2	7.733562e-9
14	C4	7.019856e-9	7.305773e-3	9.999585e-1	-5.770267e+2	8.249140e-9
15		7.078294e-9	7.333948e-3	9.999618e-1	-5.767697e+2	8.317810e-9
16		6.377318e-9	6.975820e-3	9.999572e-1	-5.780026e+2	8.000218e-9
17	C5	6.585065e-9	7.087626e-3	9.999560e-1	-5.770088e+2	8.260832e-9
18		6.751998e-9	7.173355e-3	9.999565e-1	-5.762327e+2	8.470247e-9

A2. Results for separated porosity model

A.2.1 Results for separated porosity model with variable growth material function

Table 4a. Identified parameters and fitting errors for the cases DA1–DA3, DA6, DB1–DB3, DB6, DC1–DC3, DC6

h - nucleation functions with a_1, b_1 and c_1; g - growth functions with a_2, b_2 and c_2

	Case	a_1	b_1	c_1	a_2	b_2	c_2	f
1		3.193310e-2	3.242098e-1	1.203502	8.211754e-1	4.360255e-2	2.116276e-2	3.841660e-6
2	DA1	3.940290e-2	3.785443e-1	1.289261	8.244186e-1	3.537160e-2	2.999628e-2	4.199059e-6
3		2.661606e-2	2.814220e-1	1.134062	8.396822e-1	3.000000e-2	3.000000e-2	4.568165e-6
4		3.155849e-2	3.208090e-1	1.198069	4.495204e-1	9.944665e-1	1.597589	2.070804e-6
5	DA2	3.649293e-2	3.583740e-1	1.257668	4.431633e-1	1.066636	1.629625	2.082412e-6
6		2.775885e-2	2.889782e-1	1.152616	4.461573e-1	9.958635e-1	1.690207	2.327651e-6
7		2.969356e-2	3.108419e-1	1.176169	1.811850	3.136222		1.997173e-6
8	DA3	2.694745e-2	2.877444e-1	1.139520	1.700000	3.008815		2.401137e-6
9		2.968985e-2	3.062490e-1	1.179788	1.866987	3.127403		3.184075e-6
10		3.444911e-2	3.655517e-1	1.230726	4.900660e-1	3.500000e-1		2.993737e-6
11	DA6	2.827350e-2	3.160254e-1	1.152316	6.263487e-1	2.245795e-1		4.350573e-6
12		3.122519e-2	3.359289e-1	1.187583	6.013909e-1	2.182728e-1		4.465394e-6
13		1.204609e-2	1.666148	8.675689e-1	4.641249e-1	6.000000e-1	1.241786	6.006870e-6
14	DB1	1.374453e-2	1.836789	7.450208e-1	4.951666e-1	5.437866e-1	1.370951	6.564357e-6
15		1.367317e-2	1.857122	7.407808e-1	4.815617e-1	5.631233e-1	1.426247	7.145012e-6
16		1.305251e-2	1.607246	7.859468e-1	4.891317e-1	6.762717e-1	1.312784	5.021197e-6
17	DB2	1.455673e-2	1.600000	7.178922e-1	4.666197e-1	6.000020e-1	1.400000	9.369885e-6
18		1.463789e-2	1.668226	7.365019e-1	4.729533e-1	8.868111e-1	1.291674	1.389573e-5
19		1.366112e-2	1.355215	7.220494e-1	1.096486	2.337699		3.758503e-6
20	DB3	1.822056e-2	1.364295	4.229292e-1	8.229014e-1	2.028777		5.618874e-6
21		1.682495e-2	8.920310e-1	4.481801e-1	9.370562e-1	2.158984		1.442486e-5
22		1.646760e-2	1.694600	5.892556e-1	6.141209e-1	2.284382e-1		7.968244e-6
23	DB6	1.264456e-2	1.574237	8.485074e-1	6.363586e-1	2.469675e-1		1.024005e-5
24		1.440977e-2	1.759612	6.946855e-1	6.378839e-1	2.863493e-1		1.334606e-5
25		2.249478e-2	3.419590	-2.925411	8.323893e-1	2.908707e-2	5.312087e-3	4.821597e-6
26	DC1	2.021143e-2	3.465655	-2.831718	8.166507e-1	3.000000e-2	1.274750e-2	4.869587e-6
27		1.837445e-2	3.599977	-2.795133	8.145526e-1	3.000000e-2	1.490670e-2	7.197831e-6
28		2.353712e-2	2.837932	-2.510167	4.472050e-1	8.108246e-1	1.813760	2.373988e-6
29	DC2	2.393865e-2	2.787815	-2.486816	4.484930e-1	8.125782e-1	1.791143	2.393461e-6
30		2.255554e-2	2.932520	-2.539504	4.443233e-1	8.177483e-1	1.842203	2.401889e-6
31		2.494208e-2	2.625617	-2.390641	1.725646	3.042239		2.208989e-6
32	DC3	2.440615e-2	2.633202	-2.369997	1.736362	3.077865		2.297790e-6
33		2.520594e-2	2.497748	-2.290814	1.708019	3.038395		2.314303e-6
34		2.380913e-2	2.751064	-2.449080	3.761209e-1	4.731461e-1		2.083470e-6
35	DC6	2.511742e-2	2.578891	-2.359027	4.499963e-1	4.090538e-1		2.456897e-6
36		2.569011e-2	2.580750	-2.377105	4.500000e-1	4.036821e-1		2.537421e-6

Table 4b. Statistical results for the cases DA1–DA3, DA6, DB1–DB3, DB6, DC1–DC3, DC6

s_e – standard deviation, s_{ew} – relative standard error, $r_{Y\tilde{Y}}$ – correlation coefficient, *Akaike* – AIC information-criterion, FPE – Final Prediction Error information criterion

	Case	s_e	s_{ew}	$r^n_{Y\tilde{Y}}$	$r^g_{Y\tilde{Y}}$	Akaike	FPE
1		6.773144e-8	2.251308e-2	9.994715e-1	9.975533e-1	-4.810114e+2	1.834083e-7
2	DA1	6.199115e-8	2.147680e-2	9.993504e-1	9.974684e-1	-4.782538e+2	2.004712e-7
3		1.530716e-7	3.361685e-2	9.990989e-1	9.974839e-1	-4.756420e+2	2.180930e-7
4		1.752051e-8	1.151224e-2	9.994681e-1	9.987239e-1	-5.001684e+2	9.886419e-8
5	DA2	8.428658e-9	7.992340e-3	9.994115e-1	9.987560e-1	-4.999951e+2	9.941838e-8
6		3.202048e-8	1.562876e-2	9.993415e-1	9.986667e-1	-4.965438e+2	1.111266e-7
7		1.814121e-8	1.173516e-2	9.993883e-1	9.988125e-1	-5.032907e+2	8.920376e-8
8	DA3	3.571030e-8	1.644889e-2	9.991153e-1	9.987866e-1	-4.975802e+2	1.072468e-7
9		3.651514e-8	1.658546e-2	9.994592e-1	9.988546e-1	-4.888314e+2	1.422167e-7
10		6.777280e-8	2.247722e-2	9.991662e-1	9.985657e-1	-4.907422e+2	1.337153e-7
11	DA6	1.450751e-7	3.269728e-2	9.987552e-1	9.981166e-1	-4.791549e+2	1.943184e-7
12		1.307326e-7	3.130020e-2	9.991036e-1	9.981270e-1	-4.783473e+2	1.994469e-7
13		1.910287e-7	3.865426e-2	9.968055e-1	9.990361e-1	-4.782460e+2	2.005215e-7
14	DB1	2.284232e-7	4.210737e-2	9.965694e-1	9.989954e-1	-4.653922e+2	3.035540e-7
15		2.684991e-7	4.619388e-2	9.964881e-1	9.989069e-1	-4.636360e+2	3.212476e-7
16		6.345589e-8	2.202819e-2	9.974643e-1	9.989721e-1	-4.790054e+2	1.956688e-7
17	DB2	9.466250e-8	2.634673e-2	9.977433e-1	9.988880e-1	-4.785560e+2	1.985259e-7
18		5.411387e-7	6.141882e-2	9.973998e-1	9.989997e-1	-4.779959e+2	2.021457e-7
19		8.302645e-8	2.496954e-2	9.982617e-1	9.991741e-1	-4.836898e+2	1.678736e-7
20	DB3	1.355069e-7	3.154724e-2	9.982417e-1	9.990667e-1	-4.712244e+2	2.509671e-7
21		4.169980e-7	5.424328e-2	9.963769e-1	9.991936e-1	-4.419969e+2	6.442866e-7
22		2.034398e-7	3.810506e-2	9.978735e-1	9.985452e-1	-4.698043e+2	2.627311e-7
23	DB6	4.001961e-7	5.312854e-2	9.973064e-1	9.987443e-1	-4.685968e+2	2.731668e-7
24		3.979330e-7	5.327714e-2	9.971999e-1	9.988763e-1	-4.611602e+2	3.472251e-7
25		7.346401e-8	2.328858e-2	9.993160e-1	9.977041e-1	-4.660641e+2	2.970453e-7
26	DC1	1.348016e-7	3.167064e-2	9.991350e-1	9.972233e-1	-4.607382e+2	3.527251e-7
27		3.011816e-7	4.687435e-2	9.983323e-1	9.967676e-1	-4.603084e+2	3.576495e-7
28		9.990034e-9	8.688577e-3	9.992638e-1	9.987277e-1	-4.958330e+2	1.137040e-7
29	DC2	9.153054e-9	8.319827e-3	9.992428e-1	9.987421e-1	-4.949280e+2	1.170722e-7
30		1.689490e-8	1.127949e-2	9.992833e-1	9.986803e-1	-4.947121e+2	1.178906e-7
31		1.231604e-8	9.643120e-3	9.991832e-1	9.989491e-1	-4.992190e+2	1.017245e-7
32	DC3	1.384308e-8	1.022074e-2	9.992125e-1	9.989107e-1	-4.959169e+2	1.131582e-7
33		1.667318e-8	1.121376e-2	9.991611e-1	9.989316e-1	-4.945946e+2	1.180895e-7
34		8.051829e-9	7.820902e-3	9.992443e-1	9.988906e-1	-4.998355e+2	9.972152e-8
35	DC6	1.865774e-8	1.182892e-2	9.991700e-1	9.988511e-1	-4.953665e+2	1.151853e-7
36		2.569036e-8	1.386047e-2	9.991398e-1	9.988576e-1	-4.924173e+2	1.266818e-7

A.2.2 Results for separated porosity model with constant growth material function

Table 5a. Identified parameters and fitting errors for the cases DA4, DA5, DB4, DB5, DC4, DC5

h - nucleation functions with a_1, b_1 and c_1;

g - constant growth functions with $a_2 = 1$ or a_2 estimated

	Case	a_1	b_1	c_1	a_2	f
1		2.455560e-2	2.316203e-1	1.133291	1.0	2.293625e-5
2	DA4	2.739850e-2	2.558546e-1	1.169457	1.0	2.300003e-5
3		2.802419e-2	2.644367e-1	1.177598	1.0	2.323063e-5
4		3.323955e-2	3.335458e-1	1.219735	8.581268e-1	3.856463e-6
5	DA5	3.571713e-2	3.489691e-1	1.249108	8.618957e-1	3.923766e-6
6		3.045864e-2	3.197908e-1	1.185261	8.586975e-1	4.103497e-6
7		1.078528e-2	1.835839	9.442151e-1	1.0	3.193146e-5
8	DB4	1.107597e-2	1.814623	9.133719e-1	1.0	3.225438e-5
9		1.147349e-2	1.763157	8.746320e-1	1.0	3.311483e-5
10		1.301742e-2	1.499424	7.834045e-1	8.523074e-1	6.787415e-6
11	DB5	1.562112e-2	1.507073	6.000000e-1	8.413622e-1	7.009588e-6
12		1.274083e-2	1.549482	8.242542e-1	8.474340e-1	7.597238e-6
13		3.365387e-2	2.600285	-2.711459	1.0	2.746905e-5
14	DC4	3.097063e-2	2.590565	-2.630441	1.0	2.788104e-5
15		3.412038e-2	2.488399	-2.623637	1.0	2.801906e-5
16		2.436594e-2	2.652102	-2.391388	8.588310e-1	4.491977e-6
17	DC5	2.474562e-2	2.588104	-2.352037	8.574102e-1	4.561119e-6
18		2.457036e-2	2.596011	-2.351181	8.572806e-1	4.578291e-6

Table 5b. Statistical results for the cases DA1 - DA6, DB1 - DB6, DC1 - DC6

s_e – standard deviation, s_{ew} – relative standard error, $r_{Y\tilde{Y}}$ – correlation coefficient, *Akaike* – AIC information-criterion, FPE – Final Prediction Error information criterion

	Case	s_e	s_{ew}	$r^n_{Y\tilde{Y}}$	$r^g_{Y\tilde{Y}}$	Akaike	FPE
1		3.984633e-7	5.541502e-2	9.983253e-1	9.984479e-1	-4.316202e+2	8.984245e-7
2	DA4	3.646663e-7	5.286112e-2	9.983497e-1	9.985121e-1	-4.315341e+2	9.009228e-7
3		3.227289e-7	4.958931e-2	9.985297e-1	9.984854e-1	-4.312248e+2	9.099556e-7
4		5.807169e-8	2.086283e-2	9.994689e-1	9.975623e-1	-4.848922e+2	1.612619e-7
5	DA5	4.322428e-8	1.799416e-2	9.994233e-1	9.976086e-1	-4.843558e+2	1.640762e-7
6		1.047663e-7	2.791960e-2	9.993782e-1	9.974106e-1	-4.829674e+2	1.715919e-7
7		3.445466e-7	5.036171e-2	9.952540e-1	9.984172e-1	-4.212673e+2	1.254641e-6
8	DB4	3.134510e-7	4.797997e-2	9.956229e-1	9.983613e-1	-4.206313e+2	1.280650e-6
9		3.126720e-7	4.766554e-2	9.962045e-1	9.982657e-1	-4.201004e+2	1.302771e-6
10		6.674367e-8	2.222807e-2	9.978483e-1	9.974228e-1	-4.659332e+2	2.972609e-7
11	DB5	1.408289e-7	3.198315e-2	9.982669e-1	9.971184e-1	-4.639522e+2	3.168770e-7
12		6.655629e-8	2.211882e-2	9.975321e-1	9.975790e-1	-4.441332e+2	6.005427e-7
13		3.499249e-7	5.124559e-2	9.963442e-1	9.985737e-1	-4.260972e+2	1.073632e-6
14	DC4	2.811937e-7	4.566339e-2	9.973658e-1	9.984341e-1	-4.260167e+2	1.076425e-6
15		3.069401e-7	4.786967e-2	9.966486e-1	9.985054e-1	-4.255238e+2	1.093677e-6
16		6.123366e-8	2.132040e-2	9.992148e-1	9.974423e-1	-4.808260e+2	1.838641e-7
17	DC5	6.512344e-8	2.196858e-2	9.991928e-1	9.974227e-1	-4.788617e+2	1.958915e-7
18		6.895110e-8	2.259727e-2	9.992004e-1	9.974062e-1	-4.787429e+2	1.966438e-7

A.3 Vuong test values for pairwise comparison of models

Table 6. Vuong test values for the total porosity models with varying g

Case	A2	A3	A6	B1	B2	B3	B6	C1	C2	C3	C6
A1	0.02209	-0.06799	-0.20262	0.16818	0.19988	0.15290	0.19742	0.05130	0.05499	0.03506	0.01322
A2		-0.05904	-0.04706	0.12263	0.15233	0.11057	0.14970	0.01929	-0.00057	0.00655	-0.01070
A3			0.01059	0.16068	0.19019	0.14672	0.19033	0.05715	0.06551	0.05120	0.04015
A6				0.17764	0.21069	0.16276	0.20816	0.06945	0.11982	0.06635	0.05643
B1					0.08675	-0.17144	0.06026	-0.23333	-0.17613	-0.17750	-0.18539
B2						-0.18891	-0.00407	-0.26506	-0.21470	-0.22789	-0.22978
B3							0.11309	-0.21038	-0.16030	-0.16236	-0.17001
B6								-0.24245	-0.21070	-0.21902	-0.22544
C1									-0.04325	-0.03029	-0.05706
C2										0.01689	-0.03954
C3											-0.06297

Table 7. Vuong test values for the separated porosity models with varying g

Case	DA2	DA3	DA6	DB1	DB2	DB3	DB6	DC1	DC2	DC3	DC6
DA1	-0.18582	-0.31271	-0.02360	0.07962	-0.02068	0.00887	-0.05152	0.24304	-0.18009	-0.16225	-0.17434
DA2		-0.01585	0.14398	0.14240	0.08753	0.11511	0.06497	0.29182	-0.00620	-0.04172	-0.05401
DA3			0.17238	0.17369	0.08934	0.11576	0.06835	0.31907	0.00586	-0.02957	-0.04082
DA6				0.09026	-0.01514	0.02679	-0.05501	0.61881	-0.20250	-0.20906	-0.21870
DB1					-0.08425	-0.05505	-0.12895	0.07182	-0.14938	-0.18764	-0.20869
DB2						0.20323	-0.15302	0.17924	-0.11494	-0.28684	-0.31838
DB3							-0.39121	0.14292	-0.14440	-0.30659	-0.33631
DB6								0.22079	-0.08226	-0.20654	-0.24890
DC1									-0.38567	-0.34739	-0.35460
DC2										-0.05898	-0.07226
DC3											-0.09905

Table 8. Vuong test values for the comparison of the best models from particular groups

	A5	B3	B5	C4	C6	DA3	DA6	DB3	DB6	DC6
A3	-0.01226	0.14672	0.15430	-0.00978	0.04015	0.29499	0.30367	0.27541	0.33538	0.26055
A5		0.17767	0.18444	-0.00411	0.10737	0.35998	0.37044	0.32798	0.40128	0.31560
B3			0.05309	-0.22097	-0.17001	0.12083	0.17076	0.58960	0.48022	0.19968
B5				-0.22655	-0.17844	0.09863	0.14719	0.43496	0.42353	0.17438
C4						0.37349	0.37495	0.38504	0.47157	0.37630
C6						0.36509	0.37711	0.33741	0.42854	0.33383
DA3							0.17238	0.11576	0.06835	-0.04082
DA6								0.02679	-0.05501	-0.21870
DB3									-0.39121	-0.33631
DB6										-0.24890